

Tuning the Tautomeric Behavior of Tris(Salicylaldimines)

S. Hessam M. Mehr,[†] Hiroya Oshima^{†‡}, Veronica Carta,[†] Brian O. Patrick,[†] Nicholas G. White,^{†§} and Mark J. MacLachlan^{†*}

[†] Department of Chemistry, The University of British Columbia, 2036 Main Mall, Vancouver, British Columbia V6T 1Z1, Canada

[‡] Current address: Department of Chemistry, Graduate School of Science, Nagoya University, Furo, Chikusa, Nagoya 464-8602, Japan

[§] Current address: Research School of Chemistry, Building 137, Sullivans Creek Road, The Australian National University, Canberra ACT 2601, Australia

* mmaclach@chem.ubc.ca (Prof. MacLachlan)

| | |
|---|----|
| Materials | 2 |
| Instrumentation | 2 |
| NMR Spectroscopy..... | 2 |
| X-Ray Crystallography | 2 |
| Compound 5 (CSD number: 1569188)..... | 2 |
| Compound 6 (CSD number: 1569189)..... | 5 |
| Compound 7 (CSD number: 1569190)..... | 8 |
| Compound 8 (CSD number: 1569191)..... | 10 |
| Compound 9 (CSD number: 1569192)..... | 12 |
| NMR Spectra | 15 |
| Ab initio calculations | 22 |
| Calculated UV-Vis absorption Spectra..... | 22 |
| Geometry Optimization | 22 |
| Dihedral Scans | 22 |
| Calculation of Aromatic Ring Currents and Electron Delocalization | 23 |
| Gaussian Route Sections..... | 23 |
| Energy-Optimized Atomic Coordinates | 24 |
| References..... | 24 |

Materials

All reagents and solvents were obtained from standard suppliers and used without purification. We prepared 2,4,6-triformylphloroglucinol (TFP) using the improved procedure previously reported by us.¹ The preparation of *O*-(phenylmethyl)hydroxylamine^{2,3} and pivalohydrazide⁴ was adapted from the literature.

Instrumentation

All reactions were carried out under air unless otherwise noted. High-resolution ESI mass spectra were obtained on a LCT time-of-flight (TOF) mass spectrometer. Infrared spectroscopy was carried out on an FT-IR instrument in attenuated total reflectance (ATR) mode.

NMR Spectroscopy

Unless otherwise stated, all NMR spectra were measured at 25 °C on a 400 MHz spectrometer. Direct observation of ¹³C was accomplished using a flip angle of 30° and power-gated ¹H decoupling. To speed up longitudinal relaxation, the UDEFT pulse sequence⁵ of Piotto and coworkers was used for ¹³C acquisition. We made use of ¹³C–¹H HSQC/HMBC spectra to establish atom connectivity.

Exponential window functions with line-broadening factors (LB) of 0.3 and 1.0 Hz were used for ¹H and ¹³C/¹⁹F spectra, respectively.

X-Ray Crystallography

Compound 5 (CSD number: 1569188)

Single crystal X-ray data were collected using graphite monochromated Mo K α radiation ($\lambda = 0.71073$ Å). All data were collected at 90 K to a resolution of 0.70 Å. Raw frame data (including data reduction, interframe scaling, unit cell refinement and absorption corrections) for all structures were processed using APEX2.⁶ Structures were solved using SUPERFLIP⁷ and refined using full-matrix least-squares on F^2 within the CRYSTALS suite.⁸ Hydrogen atoms were generally visible in the Fourier difference map and were initially refined with restraints on bond lengths and angles, after which the positions were used as the basis for a riding model.⁹

An initial structural determination of **5** compound suggested the presence of disorder of the entire structure over a major and minor position. In order to investigate this further, a high quality dataset was collected at 90 K using long exposure times and collecting to a resolution of 0.7 Å. The diffraction intensities and R_{merge} values were still reasonable for reflections at high angle (*e.g.* $R_{\text{merge}} \sim 0.10$ for reflections at 0.70 Å resolution).

This dataset shows that the crystal contains positional disorder over two positions (Figure S1–S3). The data were modelled by having two positions for every atom in the structure. Refinement of the occupancies of the two positions gave site occupancy factors of 0.9254(18) for the major position and 0.0746(18) for the minor position. A list of bond lengths for each of the two positions are provided in Table 1 – while the errors on the bond lengths for the minor position are relatively large (as would be expected given its very low occupancy), they still allow sensible discussion of the tautomerism (*see later*).

The major occupancy position of the molecule refined smoothly, with all non-hydrogen atoms refined anisotropically and no restraints necessary. Hydrogen atoms for this position were visible in the difference map, their positions refined, and then fixed.

The minor occupancy position of the molecule was not as well-behaved, which is unsurprising given its low occupancy. It was necessary to refine these atoms isotropically. Hydrogen atoms for this position of the molecule were inserted at geometric positions. No restraints were applied to C–C, C–N, or C–O bond lengths or angles in order to give the best possible insight into which tautomer is present – as a result, there is significant variation in bond lengths and some slightly unusual bond angles. Again, given the very low occupancy of this position, it is unsurprising that the refinement is less than ideal.

Warming the crystal used for this data collection to 230 K and collecting another dataset gave lower quality data. However, it was possible to determine that the ratio of the two disorder positions was the same, within experimental error (~ 93:7 major:minor).

The major position has consistently long C–C ring bonds [1.441(2)–1.453(2) Å] bonds, consistently short C–O bonds [1.2579(16)–1.2687(15) Å], consistently short C–C bonds coming out of the ring [1.3891(18)–1.3950(17) Å], and moderately long C–N bonds [1.3068(15)–1.3169(16) Å]. All of these bond lengths are clearly consistent with this position being the ketone-enamine tautomer.

The minor position has short C–C ring bonds, with a mean length of 1.37 Å (*cf.* 1.45 Å in the major position). The C–O bonds are long, with a mean length of 1.36 Å (*cf.* 1.26 Å in the major position) as are the C–C bonds coming out of the ring, with a mean length of 1.48 Å (*cf.* 1.39 Å in the major position). The C–N bonds are shorter in the minor position than in the major position (mean lengths: 1.28 and 1.31 Å for the minor and major position respectively). These bond lengths suggest that this minor position is the phenol-imine tautomer.

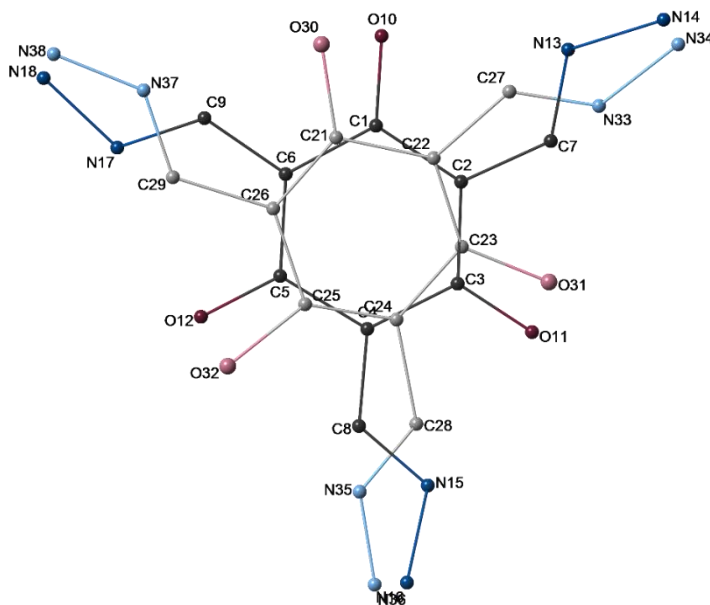


Figure S1. Overlay plot showing two disordered tautomers in the structure of **5**, as well as numbering scheme. Atoms corresponding to the major tautomer are shown darker than those of the minor tautomer. Hydrogen atoms are omitted for clarity.

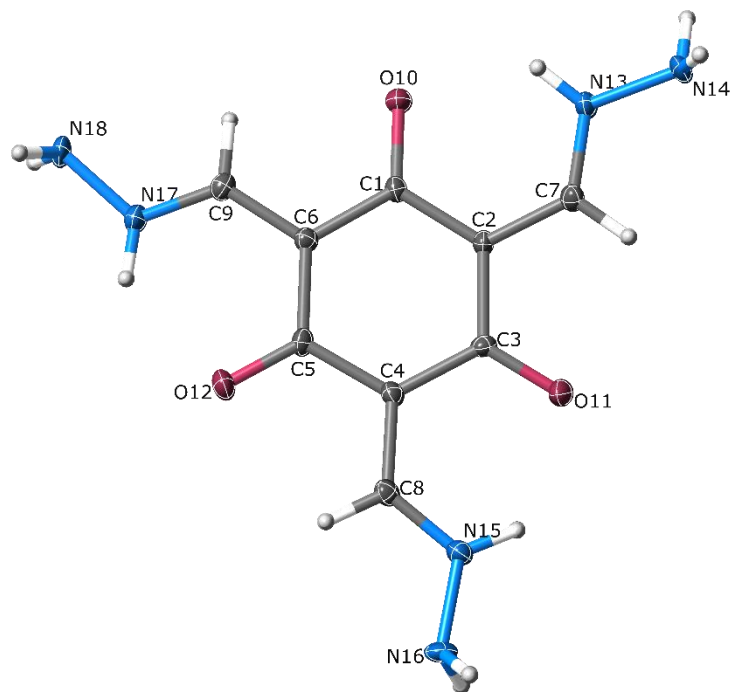


Figure S2. Thermal ellipsoid plot of the major occupancy [s.o.f.: 0.9254 (18)] tautomer of **5** (ellipsoids shown at 50% probability).

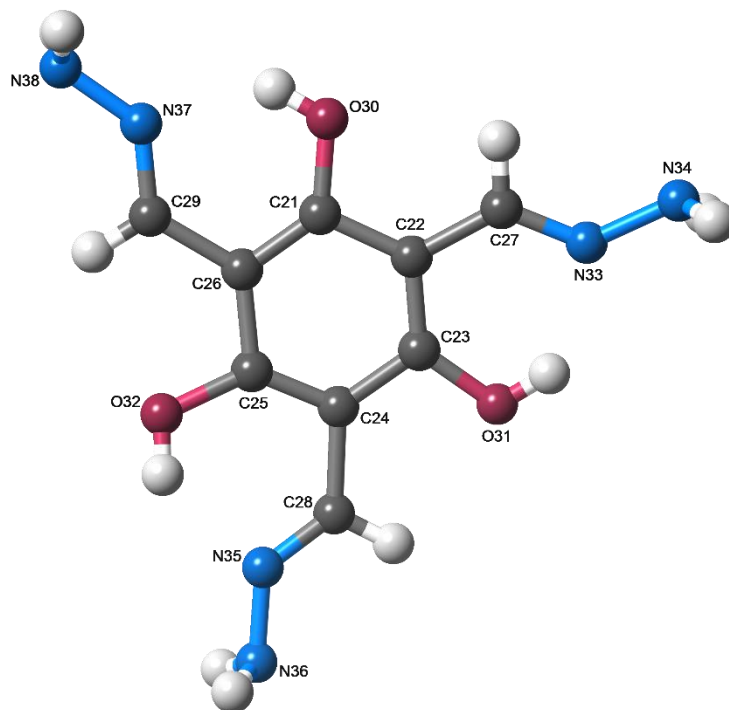


Figure S3. Structure of the minor occupancy [s.o.f.: 0.0746(18)] tautomer of **5**.

Table S1. Bond lengths for two positions of disordered structure in **5**. All bond lengths given in Å, with estimated standard deviations given in parentheses. Major position is numbered C1 through N18, minor position is numbered C21 through N38.

| Bond | Major position | Minor position |
|--|---|---|
| | [site occupancy factor: 0.9254(18)] | [site occupancy factor: 0.0746(18)] |
| 6 × Ring C–C bonds | | |
| (C1–C2, C3–C4, C5–C6 (short), C2–C3, C4–C5, C6–C1 (long) and C21–C22, C22–C23, C23–C24, C24–C25, C25–C26, C26–C21) | 1.4459(18), 1.443(2), 1.450(2), 1.4527(18), 1.453(2), 1.454(2) | 1.32(3), 1.32(3), 1.34(2), 1.39(3), 1.41(3), 1.43(3) |
| <i>Mean C–C ring bond</i> | <i>1.446(3) (long), 1.453(2) (short)</i> | <i>1.37(5)</i> |
| 3 × C–O bonds (C1–O10, C3–O11, C5–O12 and C21–O30, C23–O31, C25–O32) | 1.2579(16), 1.2605(15), 1.2687(15) | 1.335(19), 1.35(2), 1.40(3) |
| <i>Mean C–O bond</i> | <i>1.262(5)</i> | <i>1.36(4)</i> |
| 3 × C–C bonds (C2–C7, C4–C8, C6–C9 and C22–C27, C24–C28, C26–C29) | 1.3891(18), 1.3946(16), 1.3950(17) | 1.43(2), 1.49(2), 1.53(2) |
| <i>Mean C–C bond</i> | <i>1.393(3)</i> | <i>1.48(5)</i> |
| 3 × C–N bonds (C7–N13, C8–N15, C9–N17 and C27–N33, C28–N35, C29–N37) | 1.3068(15), 1.3102(16), 1.3169(16) | 1.26(2), 1.28(2), 1.30(2) |
| <i>Mean C–N bond</i> | <i>1.311(4)</i> | <i>1.28(3)</i> |

Compound 6 (CSD number: 1569189)

A colorless needle crystal of $C_{24}H_{36}N_6O_6 \cdot 2(iPrOH)$, having approximate dimensions of $0.03 \times 0.004 \times 0.004$ mm was mounted on a glass fiber. All measurements were made on a MAR300 CCD detector at the Canadian Light Source using 0.68879 \AA synchrotron radiation.

The data were collected using Mo-K α radiation at a temperature of 173.0 ± 2 K to a maximum 2θ value of 61.6° . Data were collected in a series of φ and ω scans in 1.0° oscillations using 30s exposures. The crystal-to-detector distance was 114.90 mm.

Of the 51133 reflections that were collected, 9383 were unique ($R_{int} = 0.055$); equivalent reflections were merged. Data were collected and integrated using the Bruker SAINT software package. The linear absorption coefficient, μ , for Mo-K α radiation is 0.84 cm^{-1} . Data were

corrected for absorption effects using the multi-scan technique (SADABS¹⁰), with minimum and maximum transmission coefficients of 0.689 and 0.9997, respectively. The data were corrected for Lorentz and polarization effects.

The structure was solved by direct methods.¹¹ The compound crystallizes with two molecules of solvent isopropanol in the asymmetric unit, each hydrogen bonded to a carbonyl oxygen of the main molecule. There appears to be a mixture of tautomers about the 6-membered ring. Oxygen O2 is exclusively the alcohol, O1 and O3 appear to be mixture of the two. Partially occupied hydrogen atom sites are found in sites consistent with both O—H and N—H hydrogens. All non-hydrogen atoms were refined anisotropically. All OH and NH hydrogen atoms were located in difference maps. H1, H2, H5 and H6 were refined isotropically, while H3 and H4 were refined in calculate positions. All C—H and O—H hydrogen atoms were placed in calculated positions and however were refined in calculated positions.

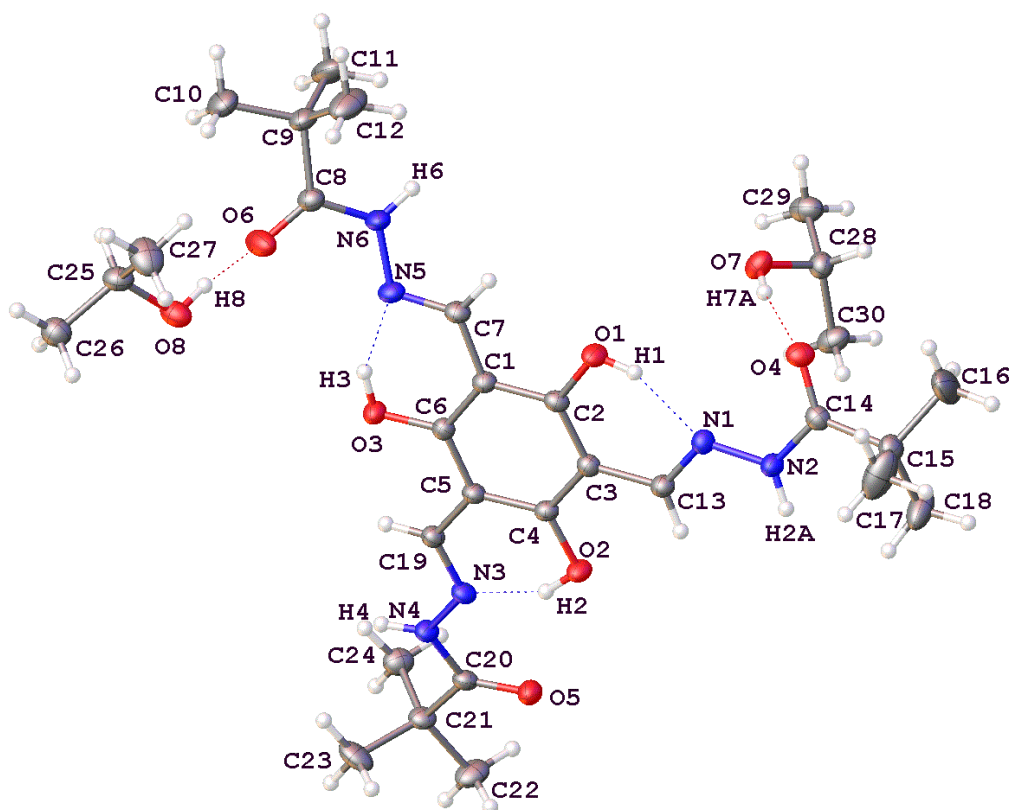


Figure S4. Thermal ellipsoids and numbering scheme for the major positions of the SCXRD for **6** with solvent molecules included.

The final cycle of full-matrix least-squares refinement (least squares function minimized: $\sum w(F_o^2 - F_c^2)^2$) on F2 was based on 9383 reflections and 451 variable parameters and converged (largest parameter shift was 0.00 times its esd) with unweighted and weighted agreement factors of:

$$R1 = \frac{\sum ||F_o| - |F_c||}{\sum |F_o|} = 0.049$$

$$wR2 = \left[\frac{\sum (w(F_o^2 - F_c^2)^2)}{\sum w(F_o^2)^2} \right]^{1/2} = 0.134$$

The standard deviation of an observation of unit weight ($[\sum w(F_o^2 - F_c^2)^2 / (N_o - N_v)]^{1/2}$ where N_o

= number of observations and N_v = number of variables) was 1.02. The weighting scheme was based on counting statistics. The maximum and minimum peaks on the final difference Fourier map corresponded to 0.48 and -0.25 e⁻/Å³, respectively.

Neutral atom scattering factors were taken from Cromer and Waber.¹² Anomalous dispersion effects were included in F_{calc}; the values for Δf' and Δf'' were those of Creagh and McAuley.¹³ The values for the mass attenuation coefficients are those of Creagh and Hubbell.¹⁴ All refinements were performed using the SHELXL-2014¹¹ via the OLEX2 interface.¹⁵

Table S2. Bond lengths for compound **6**. All bond lengths given in Å.

| Bond | Distances (Å) |
|---|---|
| 6 × Ring C–C bonds (C1–C2, C2–C3, C3–C4, C4–C5, C5–C6, C6–C1) | 1.4089(19), 1.4060(17), 1.4028(18), 1.4090(17), 1.4137(18), 1.4087(17) |
| <i>Mean C–C ring bond</i> | <i>1.4082(38)</i> |
| 3 × C–O bonds (C2–O1, C4–O2, C6–O3) | 1.3414(15), 1.3397(15), 1.3459(16) |
| <i>Mean C–O bond</i> | <i>1.342(3)</i> |
| 3 × C–C bonds (C1–C7, C3–C13, C5–C19) | 1.4429(18), 1.4519(18), 1.4506(17) |
| <i>Mean C–C bond</i> | <i>1.4485(43)</i> |
| 3 × C–N bonds (C7–N5, C13–N1, C19–N3) | 1.2845(17), 1.2879(17), 1.2853(19) |
| <i>Mean C–N bond</i> | <i>1.2859(23)</i> |

Compound 7 (CSD number: 1569190)

Single crystal X-ray data were collected using cross-coupled multilayer optics Cu-K α radiation ($\lambda = 1.54158 \text{ \AA}$). All data were collected at 90 K to a resolution of 0.80 \AA . Raw frame data (including data reduction, interframe scaling, unit cell refinement and absorption corrections) for all structures were processed using APEX2.⁶ Structures were solved using SUPERFLIP⁷ and refined using full-matrix least-squares on F^2 within the CRYSTALS suite. C–H hydrogen atoms were generally visible in the Fourier difference map and were initially refined with restraints on bond lengths and angles, after which the positions were used as the basis for a riding model, O–H hydrogen atoms were visible in the Fourier difference map and were refined with restraints on bond lengths and angles.⁹

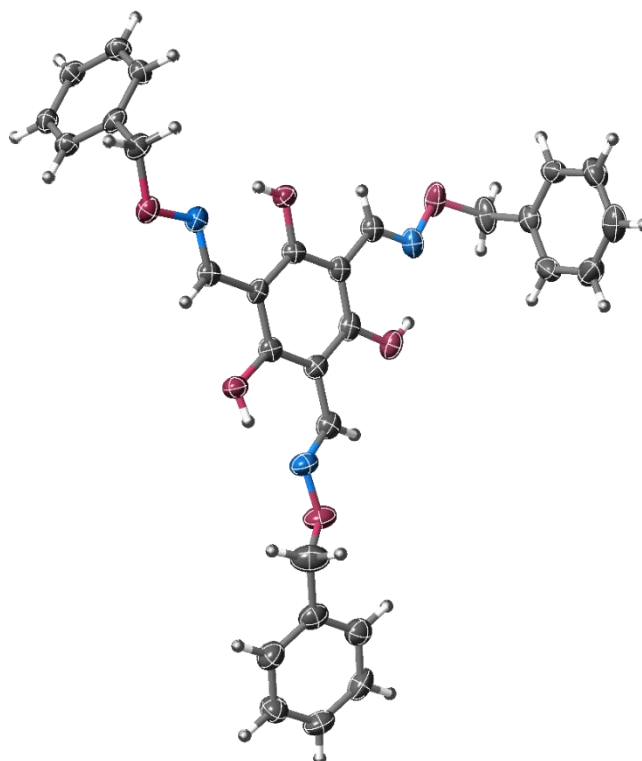


Figure S5. Thermal ellipsoid plot of **7** (thermal ellipsoids are shown at 50% occupancy).

Table S3. Bond lengths for compound **7**. All bond lengths given in \AA .

| Bond | Distances (\AA) |
|--|---|
| 6 \times Ring C–C bonds (C1–C2, C2–C3, C3–C4, C4–C5, C5–C6, C6–C1) | 1.399(4), 1.412(4), 1.411(4), 1.407(4), 1.402(4), 1.404(4) |
| <i>Mean C–C ring bond</i> | <i>1.406(6)</i> |

| | |
|--|------------------------------|
| 3 × C–O bonds (C2–O7, C4–O8, C6–O9) | 1.337(3), 1.352(4), 1.343(4) |
| <i>Mean C–O bond</i> | <i>1.344(7)</i> |
| 3 × C–C bonds (C1–C10, C3–C20, C5–C30) | 1.450(4), 1.451(4), 1.453(4) |
| <i>Mean C–C bond</i> | <i>1.451(4)</i> |
| 3 × C–N bonds (C10–N11, C20–N21, C30–N31) | 1.274(4), 1.281(4), 1.286(4) |
| <i>Mean C–N bond</i> | <i>1.280(6)</i> |

Compound 8 (CSD number: 1569191)

A yellow needle crystal of C₂₇H₆N₃O₃F₁₅, having approximate dimensions of 0.01 × 0.01 × 0.10 mm was mounted on a glass fiber. All measurements were made on a MAR300 CCD detector at the Canadian Light Source using 0.68873 Å synchrotron radiation.

The data were collected using Mo-K α radiation at a temperature of 173.0 ± 2 K to a maximum 2 θ value of 54.6°. Data were collected in a series of φ and ω scans in 1.5° oscillations using 60s exposures. The crystal-to-detector distance was 114.99 mm.

Of the 41628 reflections that were collected, 11208 were unique ($R_{\text{int}} = 0.035$); equivalent reflections were merged. Data were collected and integrated using the Bruker SAINT software package. The linear absorption coefficient, μ , for Mo-K α radiation is 1.98 cm⁻¹. Data were corrected for absorption effects using the multi-scan technique (SADABS¹⁰), with minimum and maximum transmission coefficients of 0.692 and 0.998, respectively. The data were corrected for Lorentz and polarization effects.

The structure was solved by direct methods.¹¹ The material crystallizes with two independent molecules in the asymmetric unit. Each molecule is disordered, with each site partially occupied by both keto and enol tautomers. As the difference in bond lengths between the two forms is relatively small, no restraints or constraints were employed, beyond EADP for atoms occupying the same space. In each case the keto form is present in a roughly 4:1 ratio. All non-hydrogen atoms were refined anisotropically. All N—H hydrogen atoms were located in difference maps. H1, H2, H5 and H6 were refined isotropically, while H3 and H4 were refined in calculate positions. All C—H and O—H hydrogen atoms were placed in calculated positions and however were refined in calculated positions.

The final cycle of full-matrix least-squares refinement (least squares function minimized: $\sum w(F_o^2 - F_c^2)^2$) on F2 was based on 11208 reflections and 1102 variable parameters and converged (largest parameter shift was 0.00 times its esd) with unweighted and weighted agreement factors of:

$$R1 = \sum ||F_o| - |F_c|| / \sum |F_o| = 0.034$$
$$wR2 = [\sum (w(F_o^2 - F_c^2)^2) / \sum w(F_o^2)^2]^{1/2} = 0.093$$

The standard deviation of an observation of unit weight ($[\sum w(F_o^2 - F_c^2)^2 / (N_o - N_v)]^{1/2}$ where N_o = number of observations and N_v = number of variables) was 1.10. The weighting scheme was based on counting statistics. The maximum and minimum peaks on the final difference Fourier map corresponded to 0.26 and -0.21 e⁻/Å³, respectively.

Neutral atom scattering factors were taken from Cromer and Waber. Anomalous dispersion effects were included in Fcalc; the values for $\Delta f'$ and $\Delta f''$ were those of Creagh and McAuley. The values for the mass attenuation coefficients are those of Creagh and Hubbell. All refinements were performed using the SHELXL-2014 via the Olex2 interface.

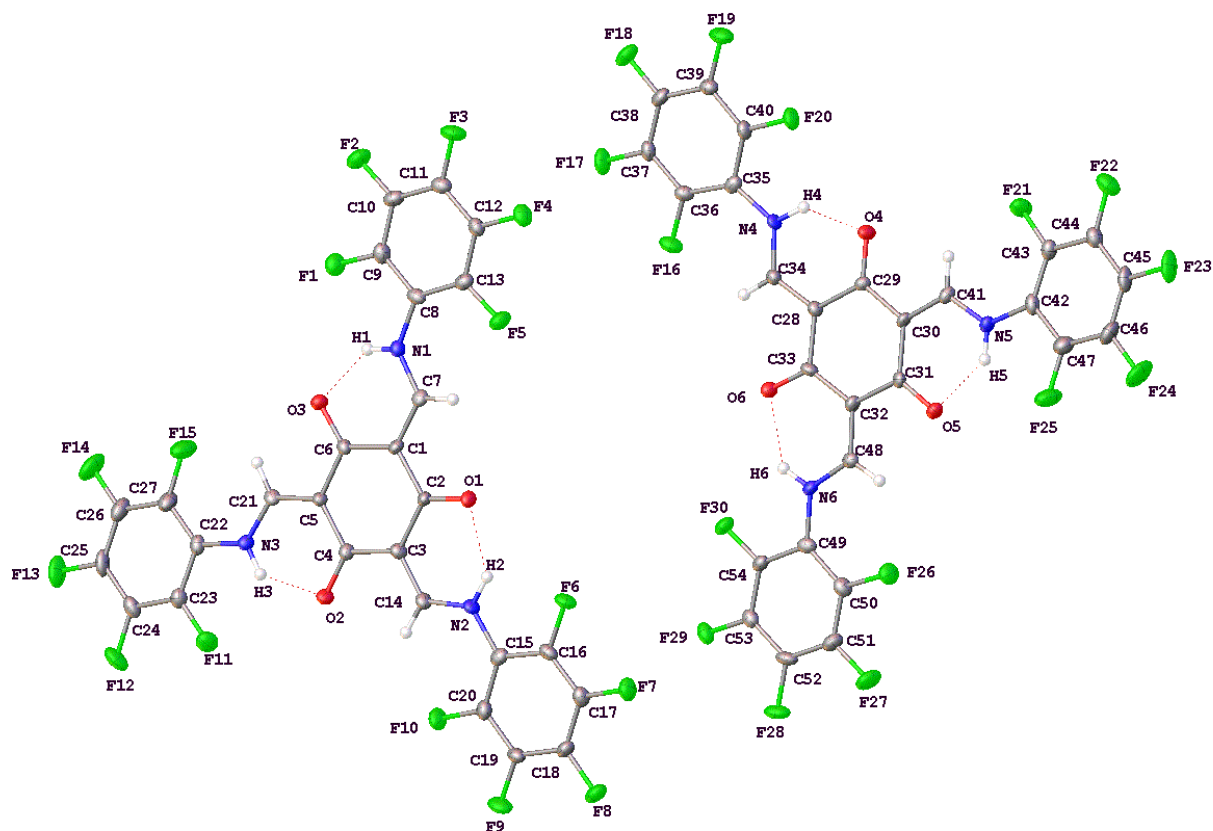


Figure S6. Thermal ellipsoid plot for the major disorder component of **8** by SCXRD (thermal ellipsoids are shown at 50% occupancy).

Table S4. Bond lengths for compound **8** (major disorder component). All bond lengths given in Å.

| Bond | Distances (Å) |
|--|---|
| 6 × Ring C–C bonds (C1–C6) | 1.464(6), 1.451(7), 1.450(6), 1.469(6), 1.449(6), 1.450(7) |
| <i>Mean C–C ring bond</i> | <i>1.458(10)</i> |
| 3 × C–O bonds (C2–O1, C4–O2, C6–O3) | 1.249(5), 1.257(5), 1.261(5) |
| <i>Mean C–O bond</i> | <i>1.256(7)</i> |
| 3 × C–C bonds (C1–C7, C3–C14, C5–C21) | 1.380(5), 1.364(6), 1.375(5) |
| <i>Mean C–C bond</i> | <i>1.373(9)</i> |

3 × C–N bonds
(C7–N1, C14–N2, C21–N3) 1.328(5), 1.333(5), 1.345(5)

Mean C–N bond *1.335(9)*

Compound 9 (CSD number: 1569192)

Single crystal X-ray data for compound **9** were collected using graphite monochromated Mo K α radiation ($\lambda = 0.71073$ Å). The data were collected at 90 K to a resolution of 0.77 Å. Raw frame data (including data reduction, interframe scaling, unit cell refinement and absorption corrections) were processed using APEX2.⁶ The structure was solved using SUPERFLIP⁷ and refined using full-matrix least-squares on F^2 within the CRYSTALS suite.⁸ Hydrogen atoms were generally visible in the Fourier difference map and were initially refined with restraints on bond lengths and angles, after which the positions were used as the basis for a riding model.⁹

The structure solved and refined in the space group P 2₁/n. One of the unit cell's angles is 90.4°, very close to 90°, but the reflections integrated poorly in an orthorhombic space group. The crystal presents pseudo-merohedral twinning, which was treated using ROTAX analysis. The structure in general doesn't show significant disorder and all the ellipsoids are relatively small. The only bond where it was necessary to add some thermal similarity and vibrational restraints is the C(5)-C(17) double bond.

The long C-C bond length in the ring [1.446(4)-1.478(1) Å], the relatively short C-O bond lengths [1.245(3)-1.250(7) Å], and short C-C bonds out of the ring [1.353(5)-1.372(1) Å], are consistent with the presence of the keto-enamine tautomer. In this structure only the keto-enamine tautomer is present.

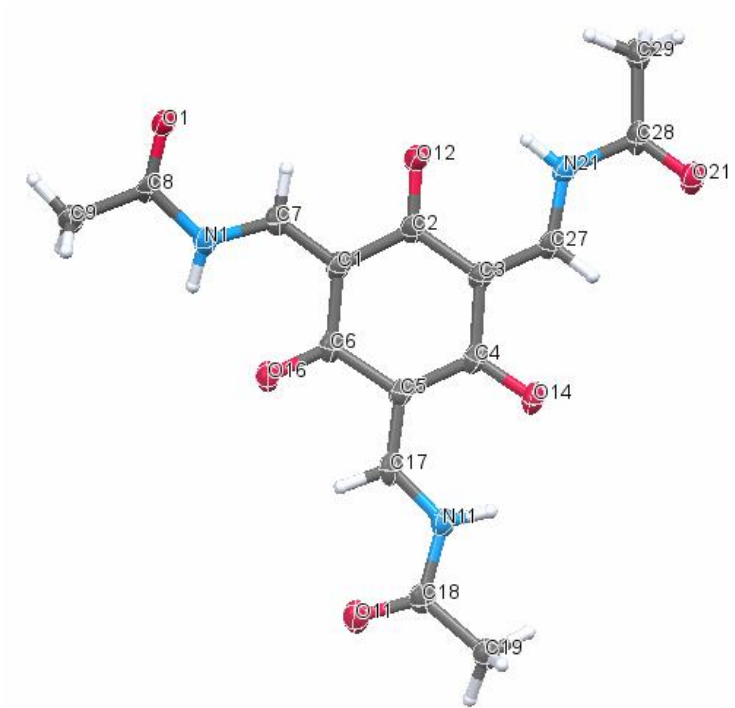


Figure S7. Thermal ellipsoid plot of **9** (thermal ellipsoids are shown at 50% occupancy).

Table S3. Bond lengths for compound **9**. All bond lengths given in Å.

| Bond | Distances (Å) |
|--|---|
| 6 × Ring C–C bonds (C1–C6) | 1.471(6), 1.447(6), 1.470(6), 1.474(6), 1.454(6), 1.478(6) |
| <i>Mean C–C ring bond</i> | <i>1.457(11) (short), 1.474(7) (long)</i> |
| 3 × C–O bonds (C6–O16, C2–O12, C4–O14) | 1.246(5), 1.249(5), 1.250(5) |
| <i>Mean C–O bond</i> | <i>1.248(5)</i> |
| 3 × C–C bonds (C1–C7, C3–C27, C5–C17) | 1.373(6), 1.367(6), 1.354(6) |
| <i>Mean C–C bond</i> | <i>1.365(10)</i> |
| 3 × C–N bonds (C7–N1, C17–N11, C27–N21) | 1.335(5), 1.340(6), 1.353(5) |
| <i>Mean C–N bond</i> | <i>1.343(9)</i> |

NMR Spectra

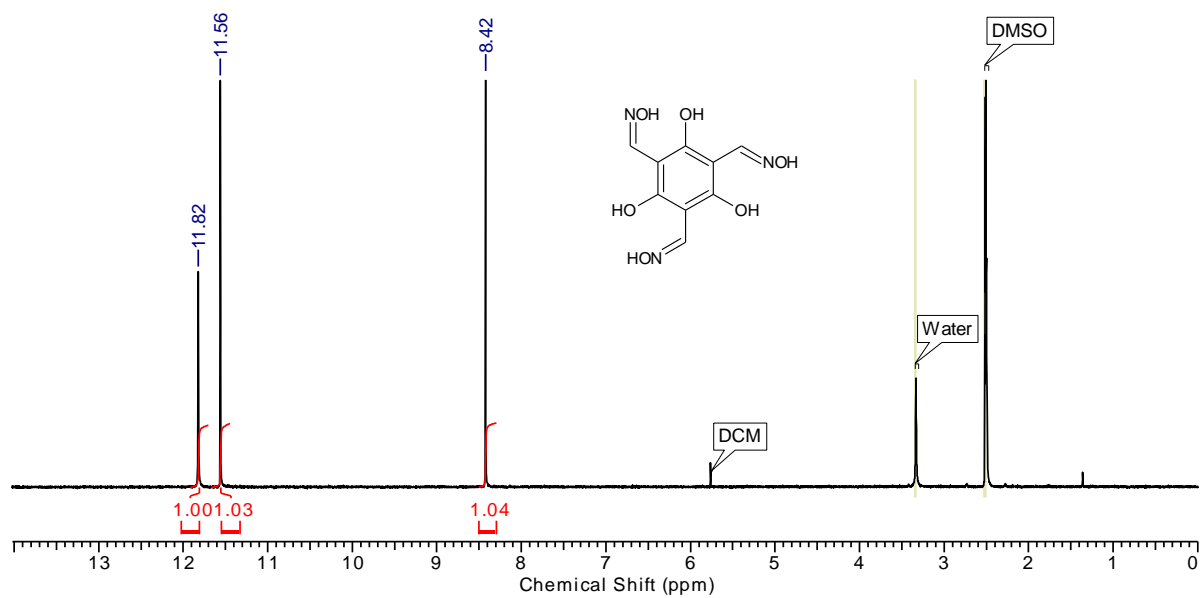


Figure S8. ^1H NMR spectrum of **4** (400 MHz, $\text{DMSO-}d_6$).

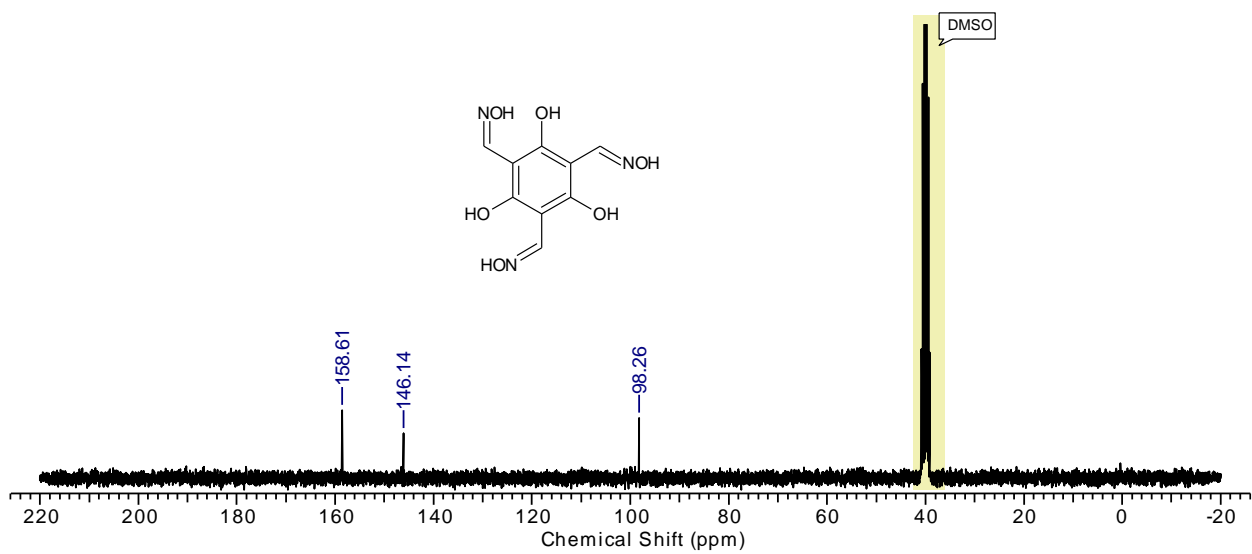


Figure S9. ^{13}C NMR spectrum of **4** (100 MHz, $\text{DMSO-}d_6$).

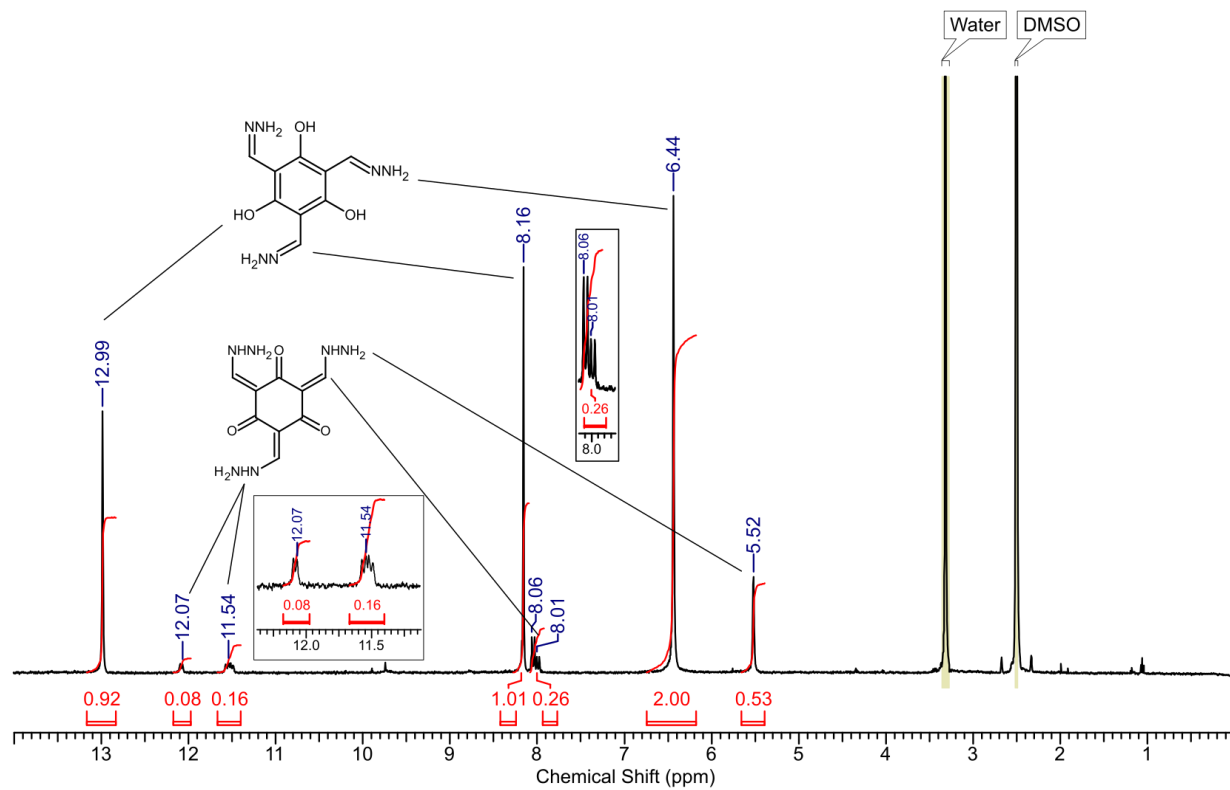


Figure S10. ¹H NMR spectrum of **5** (400 MHz, DMSO-*d*₆).

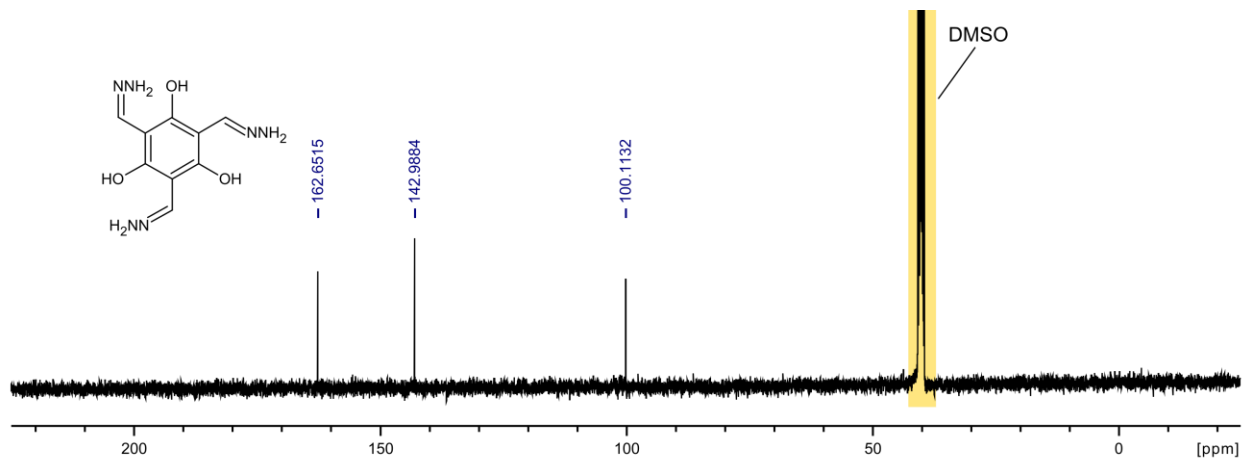


Figure S11. ¹³C NMR spectrum of **5** (100 MHz, DMSO-*d*₆).

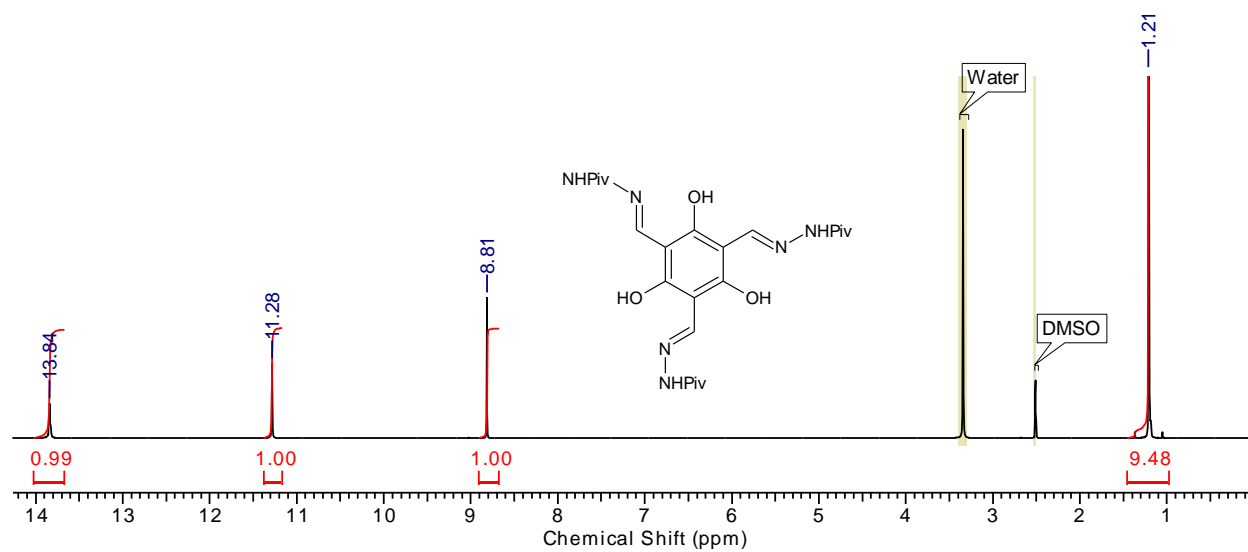


Figure S11. ^1H NMR spectrum of **6** (400 MHz, $\text{DMSO-}d_6$).

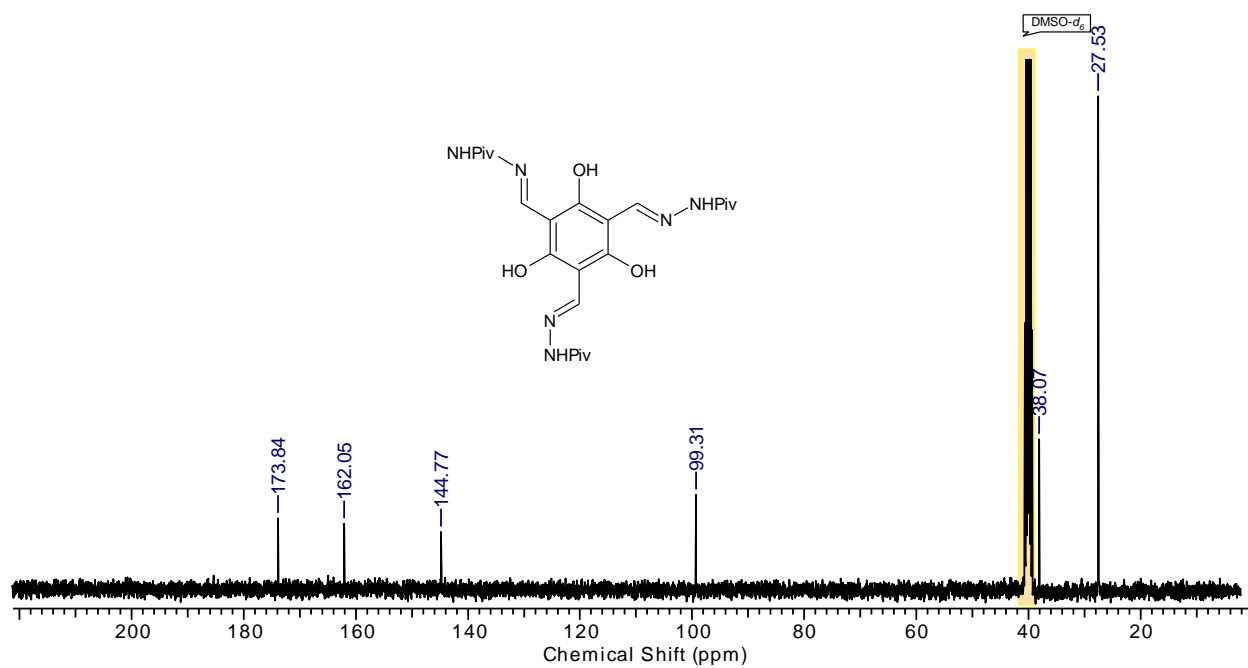


Figure S12. ^{13}C NMR spectrum of **6** (100 MHz, $\text{DMSO-}d_6$).

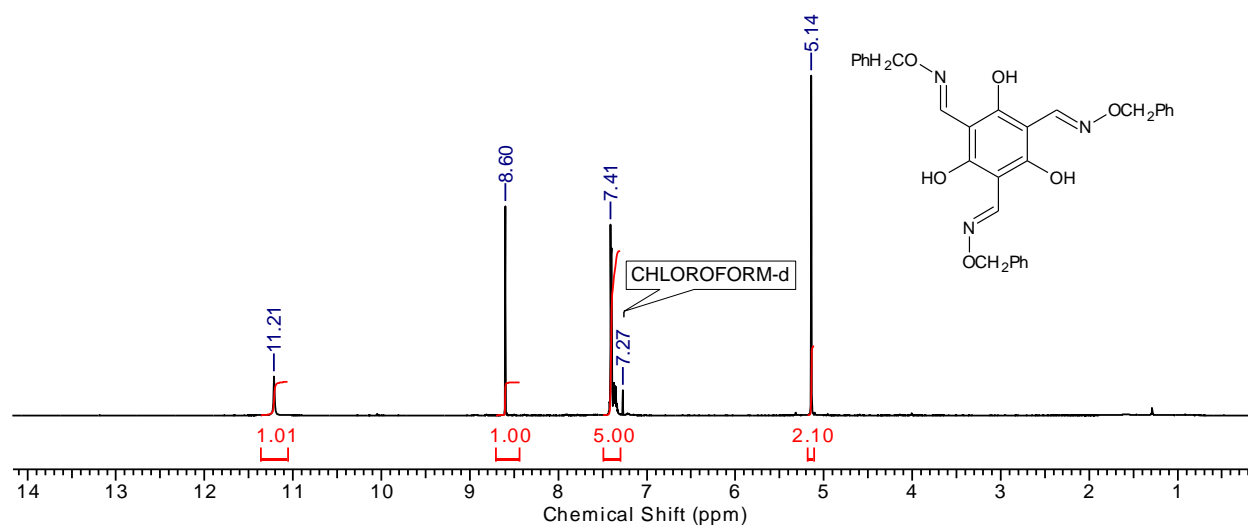


Figure S13. ^1H NMR spectrum of **7** (400 MHz, CDCl_3).

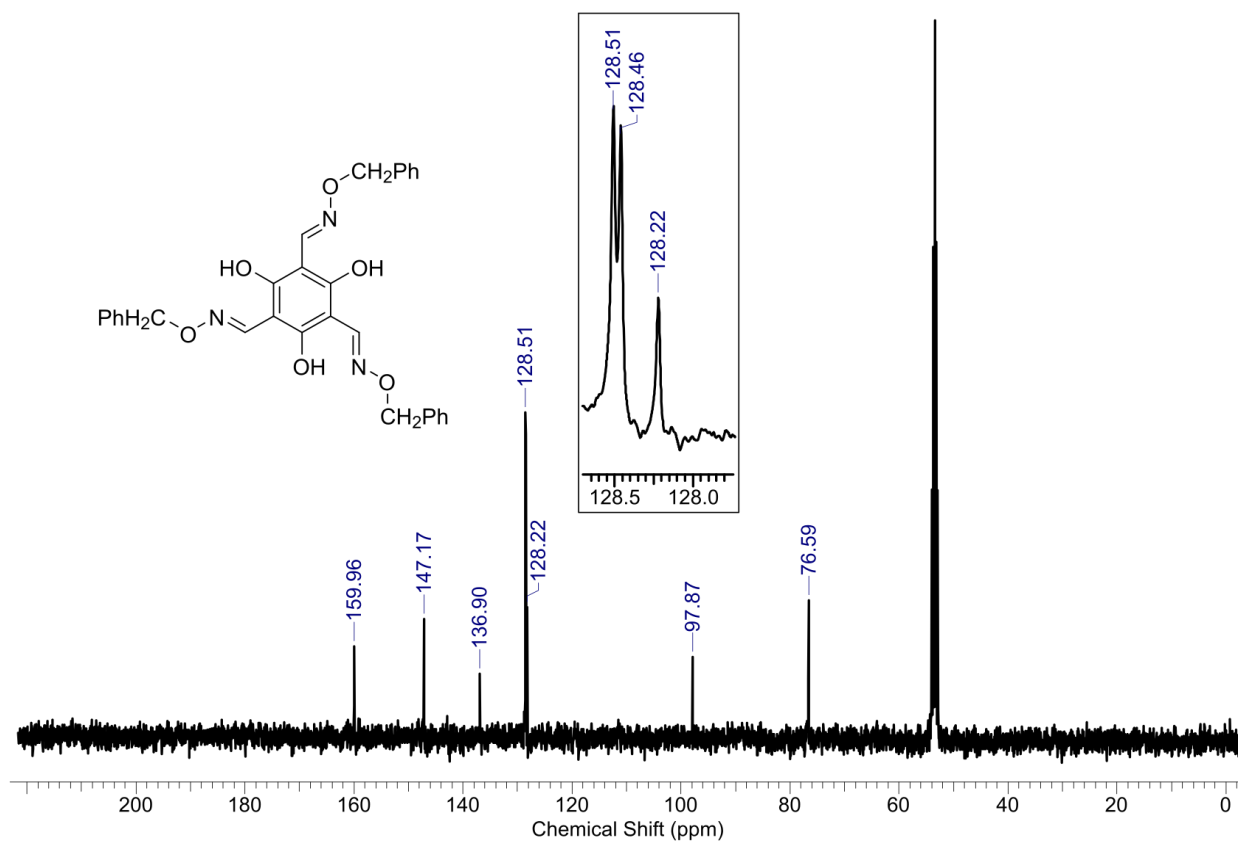


Figure S14. ^{13}C NMR spectrum of **7** (100 MHz, CD_2Cl_2).

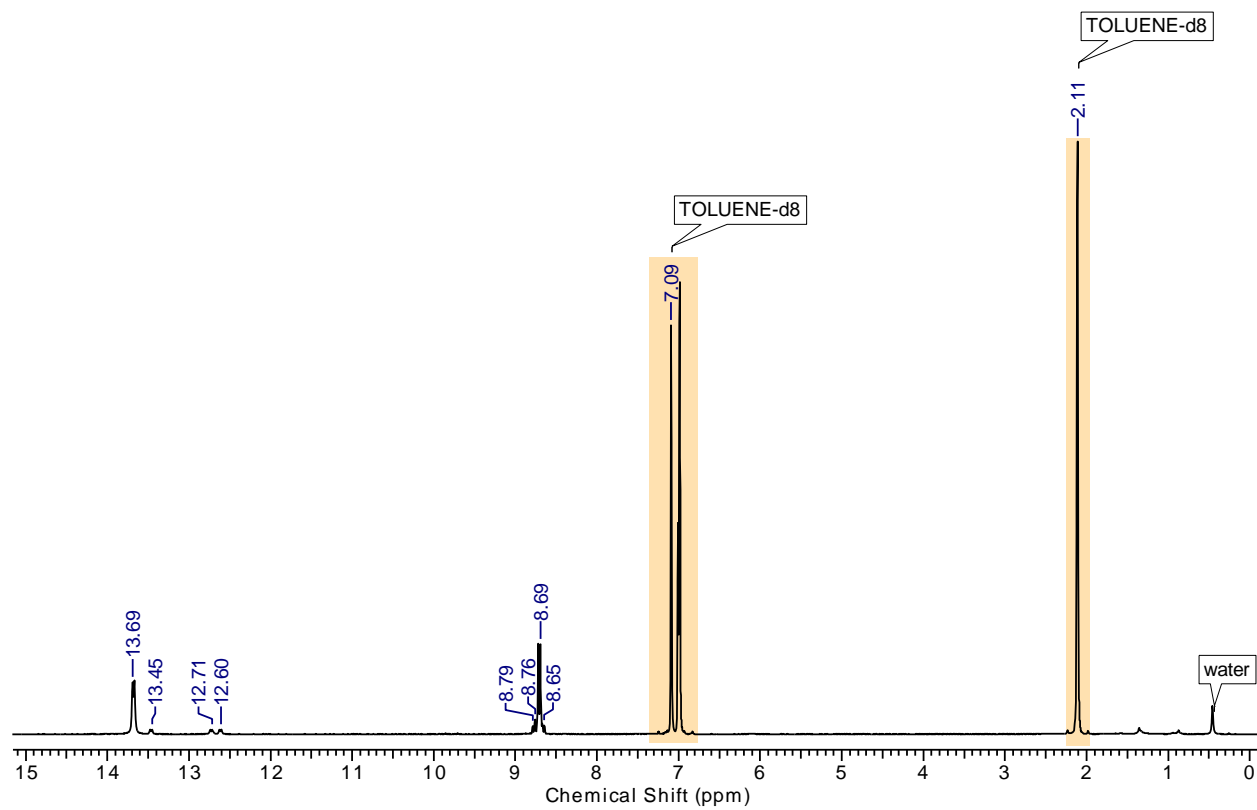


Figure S15. ^1H NMR spectrum of **8** (500 MHz, 80 $^\circ\text{C}$, $[\text{D}_8]$ Toluene).

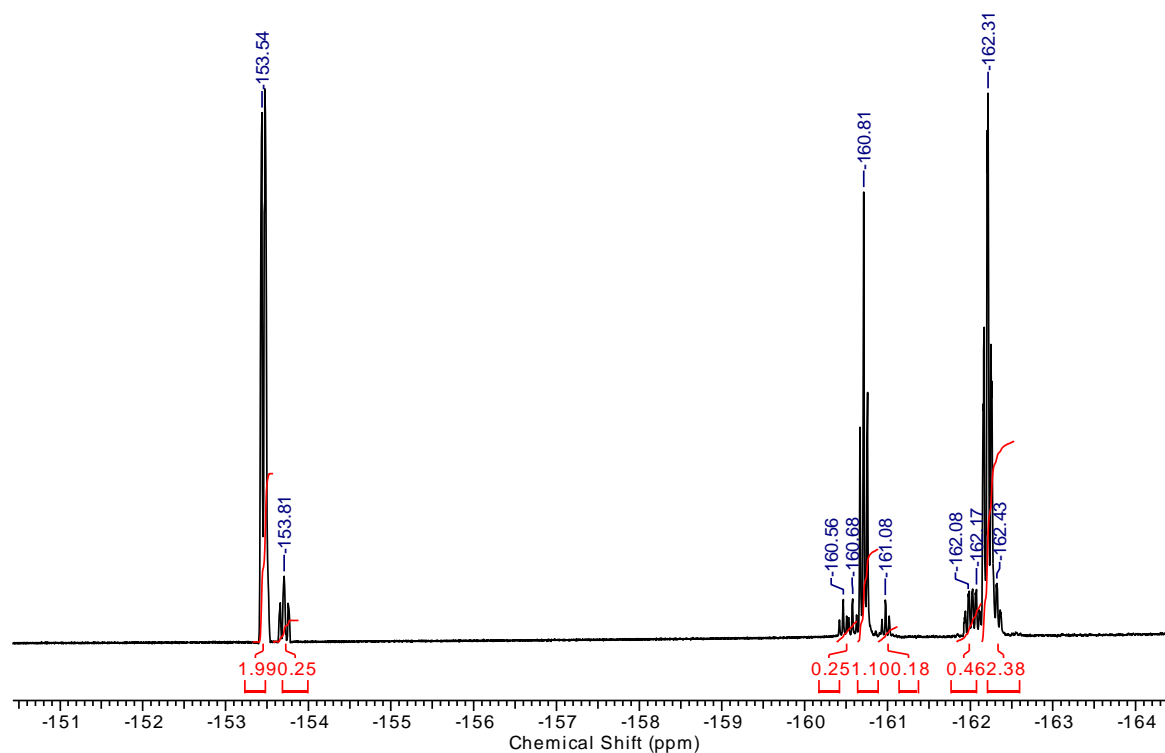


Figure S16. ^{19}F NMR spectrum of **8** (470 MHz, 80 °C, $[\text{D}_8]$ Toluene).

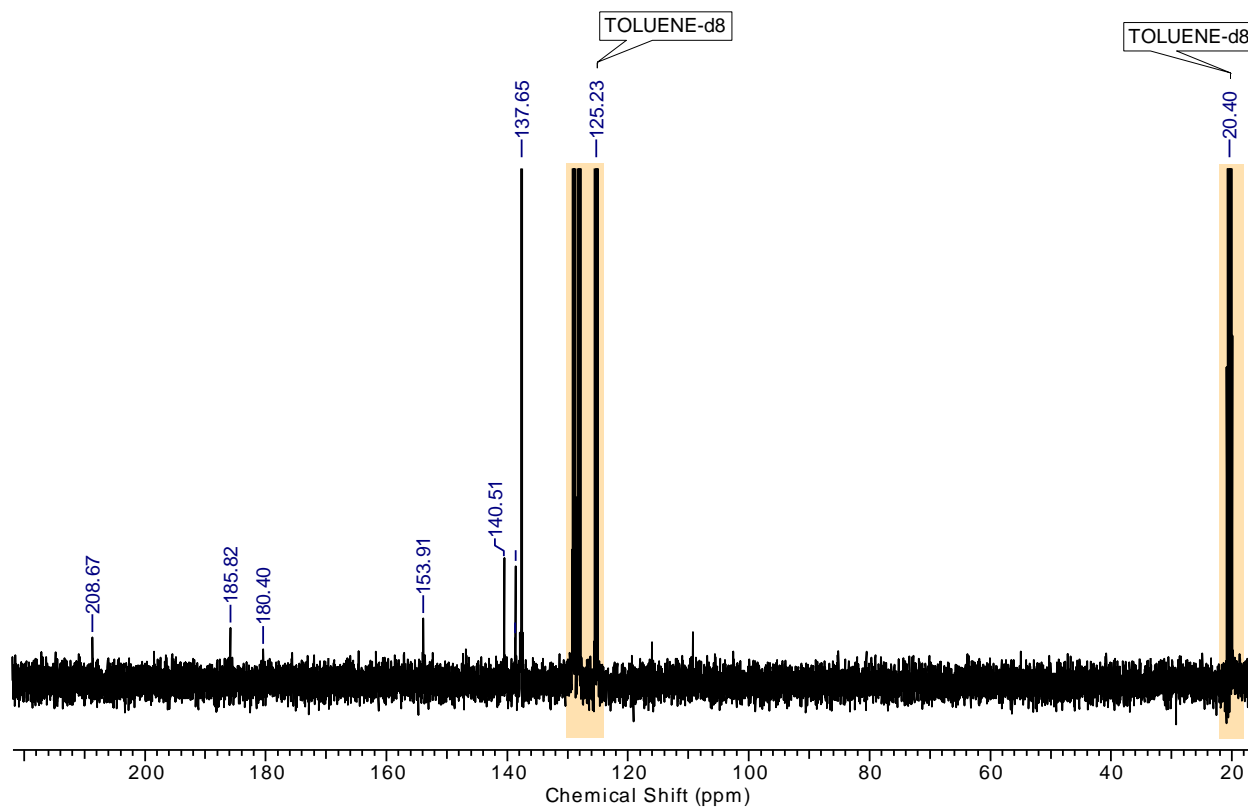


Figure S17. $^{13}\text{C}\{^1\text{H}, ^{19}\text{F}\}$ NMR spectrum of **8** (125 MHz, 80 °C, $[\text{D}_8]$ Toluene).

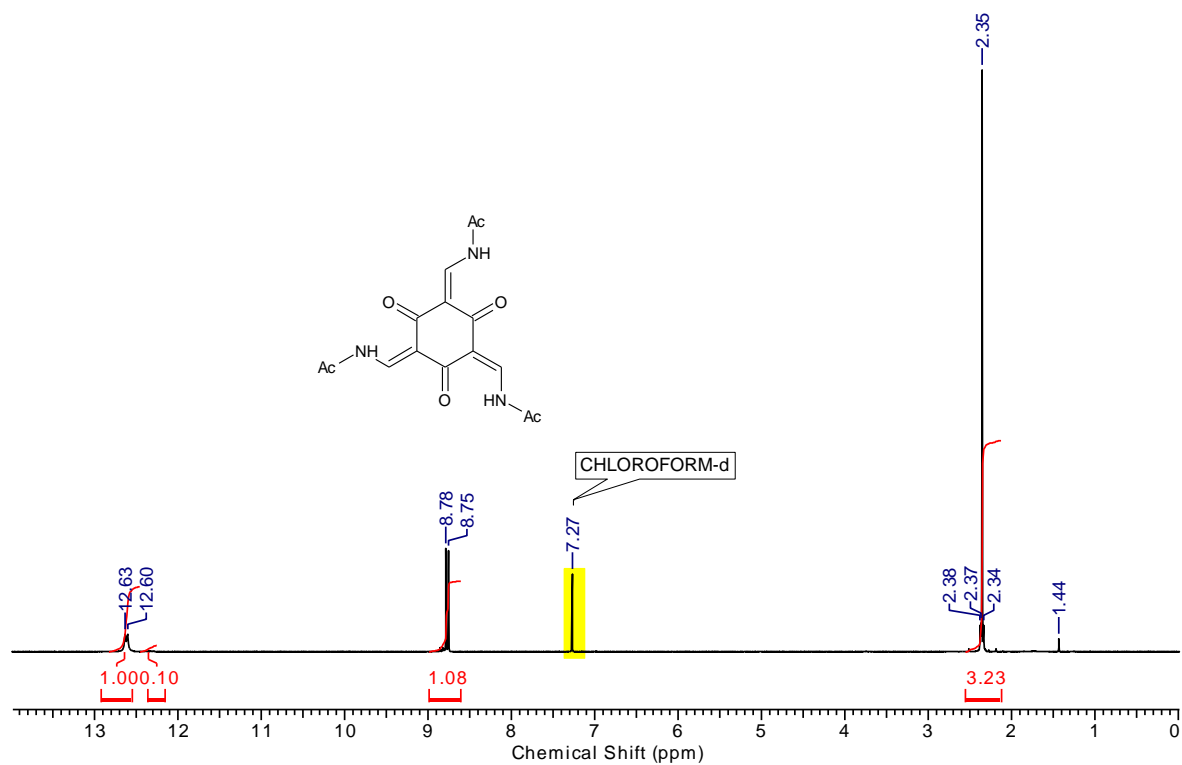


Figure S18. ^1H NMR spectrum of **9** (400 MHz, CDCl_3).

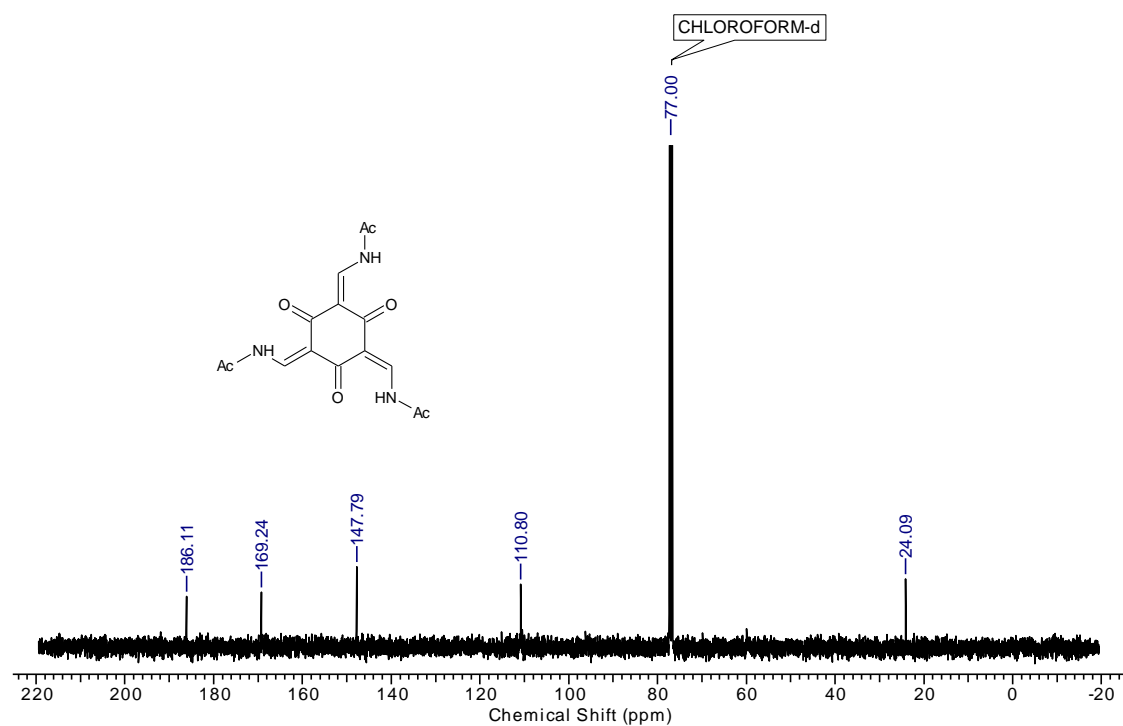


Figure S19. ^{13}C NMR spectrum of **9** (100 MHz, CDCl_3).

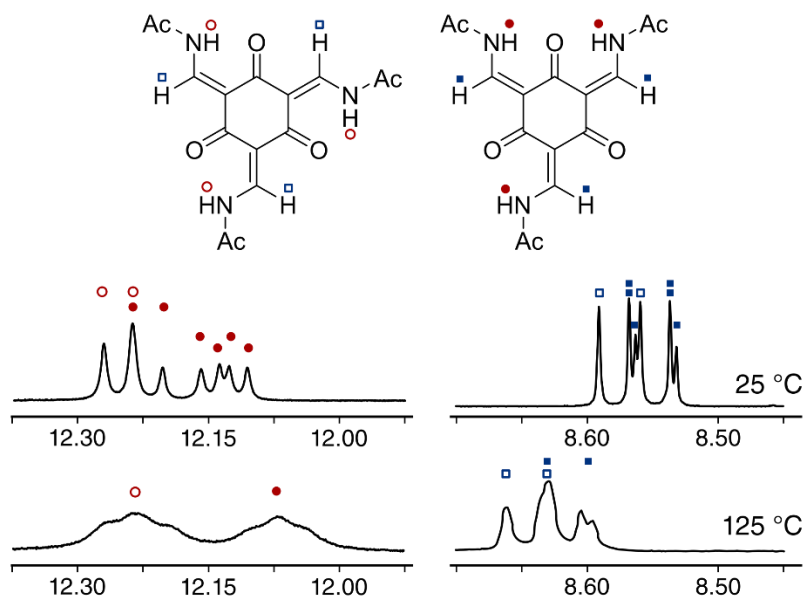


Figure S20. Variable-temperature ^1H NMR experiment for **9** (400 MHz, $\text{DMSO}-d_6$).

***Ab initio* calculations**

All *ab initio* calculations were carried out using Gaussian 09 Rev. E.¹⁶ Specifically, density functional theory (DFT) was used with the three-parameter hybrid Becke (B3LYP) functional. Structures were optimized using the 6-31+G(d,p) basis set initially before final optimization and vibrational analysis using the triple zeta basis set by Weigend and Ahlrichs (Def2TZVPP).¹⁷ For geometry optimizations, the final structure was checked for the absence of imaginary frequencies. Dihedral scans and the corresponding transition state and IRC calculations were carried out using the 6-31+G(d,p) basis set.

Calculated UV-Vis absorption Spectra

Calculated UV-Vis spectra were based on the oscillator strength obtained for singlet excited states using time-dependent density functional theory (TDDFT)¹⁸⁻²¹ with solvent modeled using the polarizable continuum method of Tomasi and coworkers.^{22,23} Calculations were performed on the gas phase energy-optimized geometry of each molecule, assuming a peak width at half-height of 2200 cm^{-1} .

Geometry Optimization

For each of **1-4**, the structures were subjected to energy optimization in the gas phase starting with the atomic coordinates from single-crystal X-ray diffraction to obtain the calculated atomic positions for the major tautomer. In each case, the minor tautomer was found by modifying the position of the H atoms in the major tautomer and performing energy optimization using the resulting atomic coordinates. All geometry optimizations were followed by vibrational analysis to ensure no imaginary frequencies were present.

Dihedral Scans

Relaxed potential energy scan calculations where the CC-CHN dihedral angle was varied in 5° increments gave reasonable energy profiles for the enol tautomers of **1** and **2**. The same procedure applied to the keto tautomer produced abrupt changes in energy around 90° torsion.

To circumvent this, a transition state was located near this dihedral angle for **1_{K-E}** and **2_{K-E}** and verified by vibrational analysis. An internal reaction coordinate (IRC) calculation was then used to allow the transition state to relax to the starting (C_{3h}) and final (C_s) geometries.

Calculation of Aromatic Ring Currents and Electron Delocalization

The Gauge-Independent Atom Orbital (GIAO) method²⁴⁻²⁶ was used in conjunction with Quantum Theory of Atoms in Molecules (QTAIM). Specifically, the GIAO wavefunctions produced by Gaussian were integrated using the AIMAll package,²⁷ giving the flux of current density between adjacent ring carbon atoms in the integration `.int` files for each atom. Interpretation is facilitated if care is taken to align the molecule with one of the Cartesian planes (e.g. xy).

Figure S21 shows the results of an example calculation comparing the diamagnetic ring current between **4_{K-E}** and **4_{E-I}**, showing the drastic reduction of I_π in the keto-enamine tautomer.

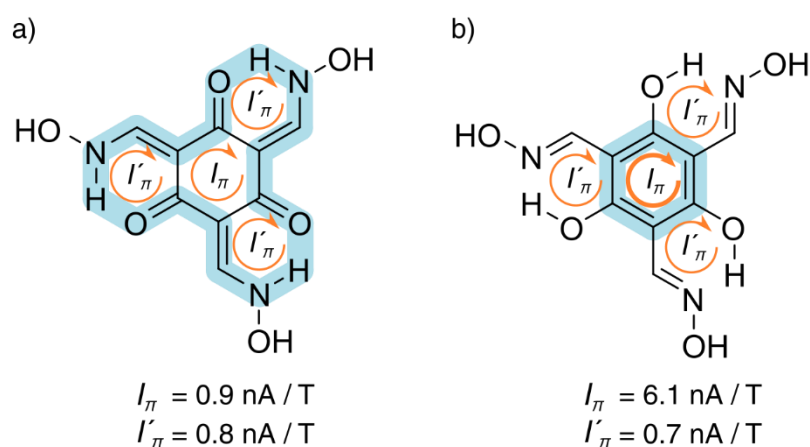


Figure S21. Comparison of diamagnetic ring current between **4_{E-I}** (a) and **4_{K-E}** (b).

The AIMAll `.sum` files also include the percentage of electron delocalization between various pairs of atoms in the molecule.

Gaussian Route Sections

- For preliminary optimizations

```
# opt RB3LYP/6-31+G(d,p) integral=grid=ultrafine
```

- For final optimizations (checkpoint containing preliminary calculation above)

```
# opt freq B3LYP/Def2TZVPP geom=allcheck guess=tcheck integral=grid=ultrafine
```

- For GIAO calculations (checkpoint containing energy-optimized coordinates)

```
# NMR=GIAO B3LYP/Def2TZVPP geom=allcheck guess=tcheck integral=grid=ultrafine
```

- For constrained geometry optimizations (dihedral scans)

```
#p opt=modredundant rb3lyp/6-31+g(d,p) geom=nodistance integral=grid=ultrafine
```

- For calculation of transition states (near the energy maximum from dihedral scan above)

```
#p opt=(calcf,ts) freq rb3lyp/6-31+g(d,p) geom=nodistance integral=grid=ultrafine
```

- For internal reaction coordinate calculations

```
#p irc=(maxpoints=90,recalc=3,stepsize=25,calcf) B3LYP/6-31+G(d,p) geom=nodistance
```

Energy-Optimized Atomic Coordinates

Energy-optimized atomic coordinates for the keto-enamine and enol-imine tautomer of **4-9** are provided online in the Protein Data Bank (PDB) format.

References

- 1 S. H. M. Mehr, H. Depmeier, K. Fukuyama, M. Maghami and M. J. MacLachlan, *Org. Biomol. Chem.*, 2017, **15**, 581–583.
- 2 J. T. Welch and K. W. Seper, *J. Org. Chem.*, 1988, **53**, 2991–2999.
- 3 T.-T. Zhao, X. Lu, X.-H. Yang, L.-M. Wang, X. Li, Z.-C. Wang, H.-B. Gong and H.-L. Zhu, *Bioorg. Med. Chem.*, 2012, **20**, 3233–3241.
- 4 K. Ohmoto, T. Yamamoto, M. Okuma, T. Horiuchi, H. Imanishi, Y. Odagaki, K. Kawabata, T. Sekioka, Y. Hirota, S. Matsuoka, H. Nakai, M. Toda, J. C. Cheronis, L. W. Spruce, A. Gyorkos and M. Wiczorek, *J. Med. Chem.*, 2001, **44**, 1268–1285.
- 5 M. Piotto, M. Bourdonneau, K. Elbayed, J.-M. Wieruszkeski and G. Lippens, *Magn. Reson. Chem.*, 2006, **44**, 943–7.
- 6 *APEX2*, Bruker AXS Inc., Madison, Wisconsin, USA, 2007.
- 7 L. Palatinus and G. Chapuis, *J. Appl. Crystallogr.*, 2007, **40**, 786–790.
- 8 P. W. Betteridge, J. R. Carruthers, R. I. Cooper, K. Prout and D. J. Watkin, *J. Appl. Crystallogr.*, 2003, **36**, 1487–1487.
- 9 R. I. Cooper, A. L. Thompson and D. J. Watkin, *J. Appl. Crystallogr.*, 2010, **43**, 1100–1107.
- 10 L. Krause, R. Herbst-Irmer, G. M. Sheldrick and D. Stalke, *J. Appl. Crystallogr.*, 2015, **48**, 3–10.
- 11 G. M. Sheldrick, *Acta Crystallogr. Sect. C Struct. Chem.*, 2015, **71**, 3–8.
- 12 D. T. Cromer and J. T. Waber, *International Tables for Crystallography*, The Kynoch Press, Birmingham, England, 1974.
- 13 D. C. Creagh and W. J. McAuley, *International Tables for Crystallography, Vol. C*, Kluwer Academic Publishers, Boston, 1992.
- 14 D. C. Creagh and J. H. Hubbell, *International Tables for Crystallography, Vol. C*, Kluwer Academic Publishers, Boston, 1992.
- 15 O. V. Dolomanov, L. J. Bourhis, R. J. Gildea, J. A. K. Howard and H. Puschmann, *J. Appl. Crystallogr.*, 2009, **42**, 339–341.
- 16 M. J. Frisch, G. W. Trucks, H. B. Schlegel, G. E. Scuseria, M. A. Robb, J. R. Cheeseman, G. Scalmani, V. Barone, B. Mennucci, G. A. Petersson, H. Nakatsuji, M. Caricato, X. Li, H. P. Hratchian, A. F. Izmaylov, J. Bloino, G. Zheng, J. L. Sonnenberg, M. Hada, M. Ehara, K. Toyota, R. Fukuda, J. Hasegawa, M. Ishida, T. Nakajima, Y. Honda, O. Kitao, H. Nakai, T. Vreven, J. A. Montgomery Jr., J. E. Peralta, F. Ogliaro, M. Bearpark, J. J. Heyd, E. Brothers, K. N. Kudin, V. N. Staroverov, R. Kobayashi, J. Normand, K. Raghavachari, A. Rendell, J. C. Burant, S. S. Iyengar, J. Tomasi, M. Cossi, N. Rega, J. M. Millam, M. Klene, J. E. Knox, J. B. Cross, V. Bakken, C. Adamo, J. Jaramillo, R. Gomperts, R. E. Stratmann, O. Yazyev, A. J. Austin, R. Cammi, C. Pomelli, J. W. Ochterski, R. L. Martin, K. Morokuma, V. G. Zakrzewski, G. A. Voth, P. Salvador, J. J. Dannenberg, S. Dapprich, A. D. Daniels, Ö. Farkas, J. B. Foresman, J. V. Ortiz, J.

- Cioslowski and D. J. Fox, *Gaussian 09*, Gaussian Inc., Wallingford, CT, 2009.
- 17 F. Weigend and R. Ahlrichs, *Phys. Chem. Chem. Phys.*, 2005, **7**, 3297.
 - 18 R. Bauernschmitt and R. Ahlrichs, *Chem. Phys. Lett.*, 1996, **256**, 454–464.
 - 19 M. E. Casida, C. Jamorski, K. C. Casida and D. R. Salahub, *J. Chem. Phys.*, 1998, **108**, 4439.
 - 20 R. E. Stratmann, G. E. Scuseria and M. J. Frisch, *J. Chem. Phys.*, 1998, **109**, 8218.
 - 21 F. Furche and R. Ahlrichs, *J. Chem. Phys.*, 2002, **117**, 7433.
 - 22 J. Tomasi, B. Mennucci and R. Cammi, *Chem. Rev.*, 2005, **105**, 2999–3093.
 - 23 G. Scalmani, M. J. Frisch, B. Mennucci, J. Tomasi, R. Cammi and V. Barone, *J. Chem. Phys.*, 2006, **124**, 94107.
 - 24 R. Ditchfield, *Mol. Phys.*, 1974, **27**, 789–807.
 - 25 R. McWeeny, *Phys. Rev.*, 1962, **126**, 1028–1034.
 - 26 K. Wolinski, J. F. Hinton and P. Pulay, *J. Am. Chem. Soc.*, 1990, **112**, 8251–8260.
 - 27 T. A. Keith, *AIMAll Rev. 16.10*, TK Gristmill Software, Overland Park, 2016.